

1990

# Phase Diagram of $UPt_3$ from Ultrasonic Velocity Measurements

Shireen Adenwalla

*University of Nebraska-Lincoln*, [sadenwalla1@unl.edu](mailto:sadenwalla1@unl.edu)

S. W. Lin

*University of Wisconsin - Milwaukee*

Q. Z. Ran

*University of Wisconsin - Milwaukee*

Z. Zhao

*Northwestern University*

J. B. Ketterson

*Northwestern University*

*See next page for additional authors*

Follow this and additional works at: <http://digitalcommons.unl.edu/physicsadenwalla>

---

Adenwalla, Shireen; Lin, S. W.; Ran, Q. Z.; Zhao, Z.; Ketterson, J. B.; Sauls, J. A.; Taillefer, L.; Hinks, D. G.; Levy, M.; and Sarma, Bimal K., "Phase Diagram of  $UPt_3$  from Ultrasonic Velocity Measurements" (1990). *Shireen Adenwalla Papers*. 4.  
<http://digitalcommons.unl.edu/physicsadenwalla/4>

This Article is brought to you for free and open access by the Research Papers in Physics and Astronomy at DigitalCommons@University of Nebraska - Lincoln. It has been accepted for inclusion in Shireen Adenwalla Papers by an authorized administrator of DigitalCommons@University of Nebraska - Lincoln.

---

**Authors**

Shireen Adenwalla, S. W. Lin, Q. Z. Ran, Z. Zhao, J. B. Ketterson, J. A. Sauls, L. Taillefer, D. G. Hinks, M. Levy, and Bimal K. Sarma

## Phase Diagram of $U\text{Pt}_3$ from Ultrasonic Velocity Measurements

S. Adenwalla,<sup>(1)</sup> S. W. Lin,<sup>(2)</sup> Q. Z. Ran,<sup>(2)</sup> Z. Zhao,<sup>(1)</sup> J. B. Ketterson,<sup>(1)</sup> J. A. Sauls,<sup>(1)</sup> L. Taillefer,<sup>(3)</sup>  
D. G. Hinks,<sup>(4)</sup> M. Levy,<sup>(2)</sup> and Bimal K. Sarma<sup>(2)</sup>

<sup>(1)</sup>*Department of Physics and Astronomy, Northwestern University, Evanston, Illinois 60208*

<sup>(2)</sup>*Department of Physics, University of Wisconsin-Milwaukee, Milwaukee, Wisconsin 53201*

<sup>(3)</sup>*Centre de Recherches sur les Très Basses Températures, CNRS, BP166X, 38042 Grenoble CEDEX, France*

<sup>(4)</sup>*Materials Science Division, Argonne National Laboratory, Argonne, Illinois 60439*

(Received 27 July 1990)

We present measurements of longitudinal ultrasonic velocity on single crystals of the heavy-fermion superconductor  $U\text{Pt}_3$ . The measurements show clear signatures of second-order phase transitions in the superconducting state, with the velocity anomalies well accounted for by Ginzburg-Landau theory. From these signatures we construct a phase diagram for  $U\text{Pt}_3$  that reveals all the boundary lines that have been identified as possible phase transitions. We are able to track the phase transition lines to a tetracritical point, located on the upper-critical-field curve, to within the width of the normal-superconducting transition.

PACS numbers: 74.30.Gn, 62.80.+f, 74.70.Tx

This Letter presents the first complete phase diagram in the field-temperature plane for the heavy-fermion superconductor  $U\text{Pt}_3$  derived from a single measurement technique.  $U\text{Pt}_3$  has shown a variety of interesting properties in the superconducting state which strongly suggest unconventional superconductivity with a multicomponent order parameter. Power-law temperature dependences of ultrasonic attenuation<sup>1-3</sup> and heat capacity<sup>4</sup> have been interpreted in terms of a gap with line or point nodes on the Fermi surface. More convincingly, a series of experiments have revealed the presence of more than one superconducting phase: Initially, ultrasonic-attenuation measurements showed the presence of two superconducting phases depending on the magnetic field;<sup>5-7</sup> subsequently, heat-capacity measurements demonstrated the presence of multiple superconducting phases even in zero field.<sup>8,9</sup> A composite phase diagram assembled from different measurements (ultrasonic-attenuation,<sup>5</sup> heat-capacity,<sup>9</sup> and torsional-oscillator data<sup>10</sup>) on different samples indicates that  $U\text{Pt}_3$  has at least two and possibly three superconducting phases. However, this interpretation relies on data from a variety of measurement techniques on samples with transition temperatures ranging from 420 to 540 mK.

Here we present measurements of ultrasonic velocity on two samples of  $U\text{Pt}_3$ . Our velocity measurements yield a more complete phase diagram for superconducting  $U\text{Pt}_3$  than has previously been available. Earlier attenuation measurements on one of the samples<sup>7</sup> (sample No. 1) revealed a peak in the attenuation (the  $H_{\text{FL}}$  peak) in field sweeps at constant temperature, as well as a peak (the  $\lambda$  peak) in temperature sweeps in low field. From these attenuation studies it was not possible to follow  $H_{\text{FL}}(T)$  very close to the upper-critical-field line  $H_{c2}(T)$ . Thus, it was not possible to answer with confidence the basic question of how many phases there are in  $U\text{Pt}_3$ . Theoretical proposals for the phase diagram of  $U\text{Pt}_3$  have been published by several authors.<sup>11-13</sup> Our results bear directly on these theories:

The phase diagrams obtained by a single measuring technique on both of the samples studied give strong support for a *tetracritical point* intersecting the upper-critical-field line, for fields both parallel and perpendicular to the  $c$  axis. In addition, the velocity anomalies at both zero-field transitions, and at  $H_{\text{FL}}$ , suggest that they are all second-order lines. Also, the magnitudes of the velocity jumps at the zero-field transitions are consistent with the Ginzburg-Landau (GL) theory for the double transition and pressure studies of  $T_c$ .

All measurements reported here were made using longitudinal sound on either sample No. 1 or No. 2. Sample No. 2 is the same crystal which was used by Hasselbach *et al.*<sup>14</sup> in their thermal-expansion measurements. The transition temperatures were 512 and 497 mK, and the transition widths were 18 and 14 mK for samples No. 1 and No. 2, respectively. Velocity measurements made on both samples revealed identical features. However, the sizes of the velocity anomalies at the various transitions were somewhat sample dependent. Sound was propagated along the  $b$  axis of sample No. 1 with the field oriented at  $45^\circ$  to the  $c$  axis. For sample No. 2, sound was propagated along the  $a$  axis and was measured for two field orientations,  $\mathbf{H}\parallel\mathbf{a}$  and  $\mathbf{H}\parallel\mathbf{c}$ .

A typical temperature sweep (Fig. 1) shows a relatively large change in velocity,  $\Delta v_{\perp}/v_{\perp} \sim -25$  ppm. The temperature of the larger velocity signature agrees with  $T_c$  obtained from susceptibility measurements to within 10 mK; subsequently, we used the velocity signature to define  $T_c$ . Note that we see no structure in the susceptibility other than the normal-superconducting transition. The slope of the velocity as a function of temperature also changes at  $T_c$ . In addition, there is a second, smaller anomaly in velocity roughly 60 mK below  $T_c$ . A very slow temperature sweep through this feature (50 mK in 5 h) reveals a small dip in the velocity of  $\sim 2$  ppm (see inset of Fig. 1). Temperature sweeps show that this lower signature shifts to lower temperatures, but closer to the upper transition line  $T_c(H)$  with increasing field.

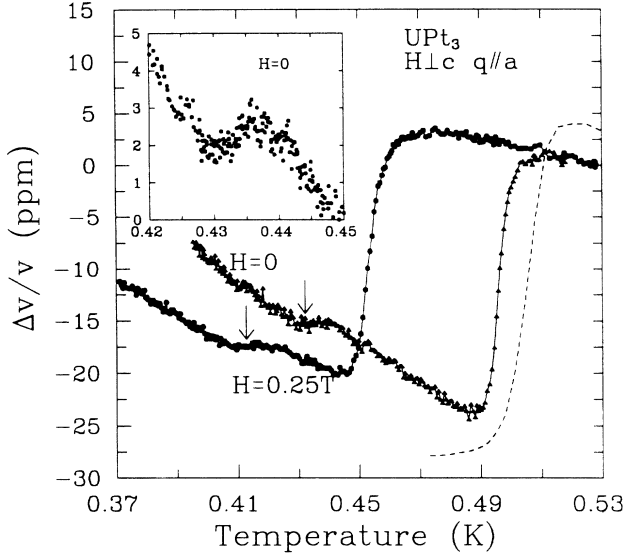


FIG. 1. Temperature dependence of the longitudinal ultrasonic velocity at  $H=0$  and  $0.25$  T. The arrows denote the second transition at  $T_{c*}$ . Inset: The result of a very slow temperature sweep through the anomaly at  $T_{c*}$ .

We identify this signature with the lower heat-capacity jump,<sup>8,9</sup> and denote this transition line by  $T_{c*}(H)$ .

The anomalies shown in Fig. 1, the discontinuities in velocity as well as slope, are characteristic signatures of second-order, mean-field transitions. The discontinuities are obtained by differentiating the GL free energy to obtain the change in the elastic moduli at the transition.<sup>15</sup> For the longitudinal mode in the basal plane the velocity jump at the normal-superconductor transition is given by

$$\frac{\Delta v_{\perp}}{v_{\perp}} = -\frac{1}{2} \frac{\Delta C}{C_n} \frac{\gamma_n}{c_{11}} \left( \frac{\partial T_c}{\partial \epsilon_{xx}} \right)^2, \quad (1)$$

where  $\Delta C/C_n$  is the relative heat-capacity jump at  $T_c$ ,  $\gamma_n$  is the normal-state heat-capacity coefficient,  $c_{11} = \rho v_{\perp}^2$  is the relevant elastic coefficient, and  $\partial T_c / \partial \epsilon_{xx}$  is the appropriate strain derivative of  $T_c$ . For zero field we can compare our measured values for  $\Delta v_{\perp} / v_{\perp}$  with the GL theory and the parameters obtained from other measurements. From Ref. 9,  $\Delta C / C_n \approx 0.47$ ,  $\gamma_n = 4.8 \times 10^6$  ergs/mole K<sup>2</sup>, and the measured elastic coefficient  $c_{11} = 3.1 \times 10^{12}$  ergs/cm<sup>3</sup>. A direct measurement of  $\partial T_c / \partial \epsilon_{xx}$  with other strains held constant is not feasible; however, this derivative can be inferred from measurements of the change in  $T_c$  under uniaxial and hydrostatic pressure. Taillefer<sup>16</sup> reports that  $T_c$  is reduced by hydrostatic and uniaxial stress along the  $c$  axis by nearly the same rate,  $\partial T_c / \partial p \approx -25$  mK/kbar, while there is no change in  $T_c$  for uniaxial stress in the basal plane. If we assume that  $T_c$  is also unaffected by volume-conserving shear stresses, then the required strain derivative can be related to the hydrostatic pressure derivative;  $\partial T_c / \partial \epsilon_{xx} \approx c_{13} \partial T_c / \partial p \approx -43$  K, where the elastic constant  $c_{13}$  has been measured in Ref. 17. With these parameters

we would expect a velocity jump of  $\Delta v_{\perp} / v_{\perp} \approx -16$  ppm, which is reasonably close to the range of measured values,  $-20$  to  $-25$  ppm.

We relate the smaller zero-field anomaly at  $T_{c*}$  to the second heat-capacity anomaly and the GL theory for the double transition.<sup>18,19</sup> Hess, Tokuyasu, and Sauls start with a two-component order parameter  $(\eta_1, \eta_2)$  belonging to one of the 2D representations of the hexagonal group. A symmetry-breaking perturbation in the normal state—quite probably the antiferromagnetic order in the basal plane—splits the 2D representation into two 1D representations with nearly degenerate transition temperatures—which we identify with  $T_c$  and  $T_{c*}$ . In addition, the GL free energy depends on two parameters,  $\beta_1$  and  $\beta_2$ , which determine the condensation energies of the two superconducting phases and the heat-capacity jumps at the two transitions. In particular, the heat-capacity measurements of the double transition in Ref. 8 imply a ratio  $\beta_2 / \beta_1 \approx 0.13$ – $0.16$ ; values closer to the weak-coupling result,  $\beta_2 / \beta_1 = 0.5$ , have also been reported.<sup>9</sup> Within this GL theory, the heat-capacity jump at the second transition can be related to that of the first transition by  $\Delta C_{c*} / T_{c*} = \Delta C / T_c (1 + \beta_2 / \beta_1)$ , which implies a velocity anomaly at  $T_{c*}$  of

$$\frac{\Delta v_{\perp}}{v_{\perp}} \Big|_{T_{c*}} = -\frac{1}{2} \frac{\beta_2}{\beta_1} \frac{\Delta C}{C_n} \frac{\gamma_n}{c_{11}} \left( \frac{\partial T_{c*}}{\partial \epsilon_{xx}} \right)^2. \quad (2)$$

The small velocity anomaly of order 10% of that at  $T_c$  is in reasonable agreement with a value of  $\beta_2 / \beta_1 \approx 0.1$ , assuming the strain derivative of the second transition temperature satisfies  $\partial T_{c*} / \partial \epsilon_{xx} \approx \partial T_c / \partial \epsilon_{xx}$ . On the other hand, if  $\beta_2 / \beta_1 \approx 0.5$  then the two strain derivatives of  $T_c$  and  $T_{c*}$  differ by a factor of  $\sim 2$ – $3$ .

A similar calculation predicts substantially larger velocity anomalies for longitudinal sound propagating along the  $c$  axis, e.g., at  $T_c$ ,

$$\frac{\Delta v_{\parallel}}{v_{\parallel}} = -\frac{1}{2} \frac{\Delta C}{C_n} \frac{\gamma_n}{c_{33}} \left( \frac{\partial T_c}{\partial \epsilon_{zz}} \right)^2 \approx -48 \text{ ppm}. \quad (3)$$

An analysis can also be made of the discontinuities in the slopes of the velocities (which depend on strain derivatives of both  $T_c$  and the heat-capacity anomaly). Uniaxial-stress measurements of changes in  $T_c$  combined with precision velocity measurements such as these could be used to obtain precise, noncalorimetric measurements of the heat-capacity anomalies at  $T_c$  and  $T_{c*}$ .

Anomalies in the velocity are also observed by sweeping the field. Earlier sound-attenuation measurements<sup>5,6</sup> led to a number of speculations that the attenuation peak at  $H_{FL}$  represented a structural transition of the flux lattice induced by a change in an underlying unconventional order parameter,<sup>20</sup> or a vortex-core transition,<sup>7,12</sup> again related to an unconventional order parameter. Recently, a concrete example of a high-field transition was obtained within the GL theory for an unconventional order parameter appropriate for hexagonal symmetry (in

particular, one of the two-dimensional representations).<sup>21</sup> In this theory of the transition a lattice of *doubly quantized* vortices is stable below  $H_{FL}$ , while at high fields,  $H_{FL} < H < H_{c2}$ , the stable lattice is a more conventional lattice of singly quantized vortices. Numerical solutions of the GL equations show a dissociation transition at  $H \approx 0.5H_{c2}$  for  $H \parallel c$ .<sup>21</sup>

The field sweep shown in Fig. 2 reveals a sharp dip in the velocity,  $\Delta v_{FL}/v_{FL} \approx 3$  ppm (and a change in slope), at the position of the previously measured  $H_{FL}$  peak, again indicative of a second-order transition. The signature at  $H_{c2}$  is also clearly visible. Field sweeps at higher temperatures show a shift of  $H_{FL}$  to lower fields. The  $H_{FL}$  signature was also observed in temperature sweeps at higher temperatures where  $dH_{FL}/dT$  is steepest. No similar anomalies were observed in transverse-sound measurements.

The phase diagram for  $UPT_3$  based on velocity measurements is shown in Fig. 3. It reveals all of the known signatures that have been previously identified as possible phase transitions. The inset of Fig. 3 shows  $T_{c*}(H)$  and  $T_c(H)$ , obtained from our velocity signatures, compared with the data of Ref. 9 obtained from heat-capacity measurements. The velocity signatures remain sharp and unambiguous to within the width of the transition at  $H_{c2}$  [or  $T_c(H)$ ] and as a result lead to several important conclusions.

(i) The data provide strong support for the interpretation that both transition lines,  $H_{FL}(T)$  and  $T_{c*}(H)$ , intersect the upper-critical-field curve, thus dividing the mixed state into *three distinct phases*; the transition lines are not different segments of the same phase boundary as proposed by Joynt.<sup>11</sup>

(ii) Within the limits (see below) of our resolution, which is the width of the normal-superconducting transition, the three phase lines [ $H_{FL}(T)$ ,  $T_{c*}(H)$ , and  $H_{c2}(T)$ ] intersect at a tetracritical point, for field directions both along the  $c$  axis and in the basal plane. For  $H$  in the basal plane, we observe a kink in  $H_{c2}(T)$  (Refs. 16 and 22) at the tetracritical point, whereas we see no such

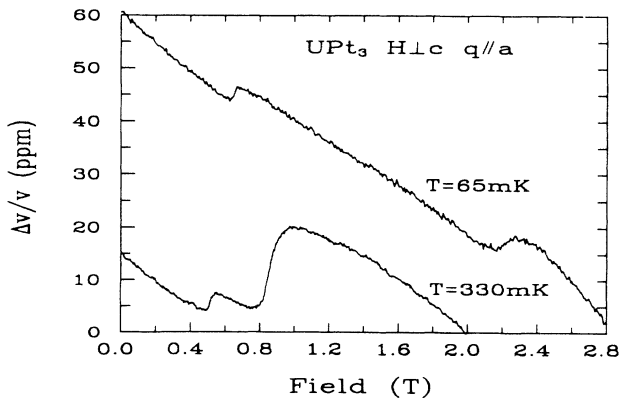


FIG. 2. Magnetic-field dependence of the longitudinal ultrasonic velocity. The signatures at  $H_{FL}$  and  $H_{c2}$  are both clearly visible.

indication for fields at  $45^\circ$  or  $90^\circ$  from the basal plane.

(iii) The tetracritical point moves to lower fields as the field is rotated away from the  $c$  axis into the basal plane. For  $H \parallel c$ , the lines meet at 9.5 kG; for  $H$  at  $45^\circ$  to the  $c$  axis, the tetracritical point shifts to 5.7 kG; and for  $H \parallel a$ , to 4.7 kG. Likewise, the slope of  $H_{FL}(T)$  near the tetracritical point varies from  $-1.87$  T/K for fields along the  $c$  axis to  $-0.77$  T/K for fields in the basal plane, with an intermediate value of  $-0.88$  T/K for  $H$  at  $45^\circ$  to the  $c$  axis.

How good is the identification of a tetracritical point? Within the limits of our resolution, the three phase lines [ $H_{FL}(T)$ ,  $T_{c*}(H)$ , and  $H_{c2}(T)$ ] intersect at a tetracritical point. If, instead, we assume that  $H_{FL}(T)$  and  $T_{c*}(H)$  are *different* segments of the same transition

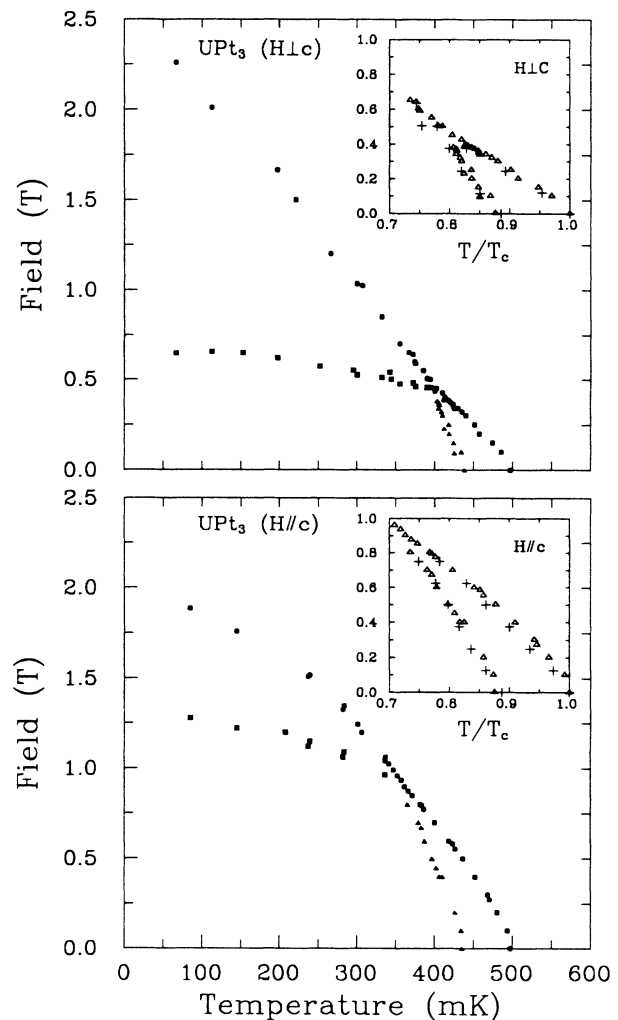


FIG. 3. Phase diagrams obtained from velocity measurements for three different orientations of the field:  $H \perp c$  and  $H \parallel c$ . The data points for the phase boundaries are denoted as  $\blacksquare$ ,  $H_{FL}$ ;  $\bullet$ ,  $H_{c2}$ ; and  $\blacktriangle$ ,  $T_{c*}$ . The insets show our results for  $T_{c*}(H)$  and  $H_{c2}(T)$  from velocity measurements ( $\Delta$ ) in comparison with the heat-capacity data of Refs. 9 and 16 (shown as +). Note that we have normalized the temperature scales in the insets for the different samples.

line, and therefore continuous, then this phase boundary would have to approach the upper-critical-field line to within 12–15 mK without intersection. Similarly, we can put a constraint on the phase diagram proposed by Blount, Varma, and Aeppli,<sup>13</sup> who argue that the two transition lines,  $H_{FL}(T)$  and  $T_{c^*}(H)$ , intersect the upper critical field at different points (for  $\mathbf{H} \perp \mathbf{c}$ ). We can rule out two tricritical points for  $\mathbf{H} \perp \mathbf{c}$ , unless their separation along  $H_{c2}$  is less than  $\delta H \approx 0.07$  T and  $\delta T \approx 18$  mK. Careful examination of the slopes of the transition lines  $H_{FL}(T)$  and  $T_{c^*}(H)$  near  $H_{c2}$  favors a tetracritical point for both  $\mathbf{H} \perp \mathbf{c}$  and  $\mathbf{H} \parallel \mathbf{c}$ . This result is supported by the recent analysis of Yip, Li, and Kumar<sup>23</sup> on thermodynamic constraints for the possible  $H$ - $T$  phase diagrams of  $\text{UPt}_3$ . These authors show that certain phase diagrams are not allowed by thermodynamics. A tricritical point at which three second-order transitions meet is not allowed; if three second-order transition lines meet at a point, then an additional phase transition line, which can be either first- or second-order, must emerge from the same point; i.e., it must be a tetracritical point. Yip, Li, and Kumar then place constraints on the slopes of the transition lines. The new data for these phase boundaries warrant a careful examination of the consistency relations for a tetracritical point.

The work at University of Wisconsin–Milwaukee was supported by the Office of Naval Research. The work of S.A., Z.Z., and J.B.K. at Northwestern University was supported by the National Science Foundation under Grant No. DMR-89-07396. The work of J.A.S. was supported by the National Science Foundation through the Northwestern University Materials Research Center Grant No. DMR-8821571. We also thank Sungkit Yip for providing us with a copy of Ref. 23 prior to publication, and Dierk Rainer for his comments on the paper.

*Note added.*—After this work was completed we learned of similar measurements by Bruls *et al.*<sup>24</sup>

<sup>1</sup>D. J. Bishop, C. M. Varma, B. Batlogg, E. Bücher, Z. Fisk, and J. L. Smith, Phys. Rev. Lett. **53**, 1009 (1984).

<sup>2</sup>V. Müller, D. Maurer, E. W. Scheidt, C. Roth, K. Lüders, E. Bücher, and H. E. Bömmel, Solid State Commun. **57**, 319

(1986).

<sup>3</sup>B. S. Shivaram, Y. H. Jeong, T. F. Rosenbaum, and D. G. Hinks, Phys. Rev. Lett. **56**, 1078 (1986).

<sup>4</sup>A. Sulpice, P. Gandit, J. Chaussy, J. Flouquet, D. Jaccard, P. Lejay, and J. L. Tholence, J. Low Temp. Phys. **62**, 39 (1986).

<sup>5</sup>Y. J. Qian, M.-F. Xu, A. Schenstrom, H.-P. Baum, J. B. Ketterson, D. G. Hinks, M. Levy, and B. K. Sarma, Solid State Commun. **63**, 599 (1987).

<sup>6</sup>V. Müller, C. Roth, D. Maurer, E. W. Scheidt, K. Lüders, E. Bücher, and H. E. Bömmel, Phys. Rev. Lett. **58**, 1224 (1987).

<sup>7</sup>A. Schenstrom, M.-F. Xu, Y. Hong, D. Bein, M. Levy, B. K. Sarma, S. Adenwalla, Z. Zhao, T. A. Tokuyasu, D. W. Hess, J. B. Ketterson, J. A. Sauls, and D. G. Hinks, Phys. Rev. Lett. **62**, 332 (1989).

<sup>8</sup>R. A. Fisher, S. Kim, B. F. Woodfield, N. E. Phillips, L. Taillefer, K. Hasselbach, J. Flouquet, A. L. Giorgi, and J. L. Smith, Phys. Rev. Lett. **62**, 1411 (1989).

<sup>9</sup>K. Hasselbach, L. Taillefer, and J. Flouquet, Phys. Rev. Lett. **63**, 93 (1989).

<sup>10</sup>R. N. Kleiman, P. L. Gammel, E. Bücher, and D. J. Bishop, Phys. Rev. Lett. **62**, 328 (1989).

<sup>11</sup>R. Joynt, Supercond. Sci. Technol. **1**, 210 (1988).

<sup>12</sup>T. A. Tokuyasu, D. W. Hess, and J. A. Sauls, Phys. Rev. B **41**, 8891 (1990).

<sup>13</sup>E. I. Blount, C. M. Varma, and G. Aeppli, Phys. Rev. Lett. **64**, 3074 (1990).

<sup>14</sup>K. Hasselbach, A. Lacerda, A. de Visser, K. Behnia, L. Taillefer, and J. Flouquet (to be published).

<sup>15</sup>L. R. Testardi, Phys. Rev. B **3**, 95 (1971).

<sup>16</sup>L. Taillefer, Physica (Amsterdam) **163B**, 278 (1990).

<sup>17</sup>A. de Visser, J. J. M. Franse, A. Menovsky, and T. T. Palstra, J. Phys. F **15**, L53 (1985).

<sup>18</sup>D. W. Hess, T. A. Tokuyasu, and J. A. Sauls, J. Phys. Condens. Matter **1**, 8135 (1989).

<sup>19</sup>K. Machida and M. Ozaki, J. Phys. Soc. Jpn. **58**, 2244 (1989).

<sup>20</sup>G. E. Volovik, J. Phys. C **21**, L221 (1988).

<sup>21</sup>T. A. Tokuyasu and J. A. Sauls, Physica (Amsterdam) **165-166B**, 347 (1990).

<sup>22</sup>U. Rauchschwalbe, Physica (Amsterdam) **147B**, 1 (1987).

<sup>23</sup>S. K. Yip, T. Li, and P. Kumar (to be published).

<sup>24</sup>G. Bruls, D. Weber, B. Wolf, P. Thalmeier, B. Lüthi, A. de Visser, and A. Menovsky, preceding Letter, Phys. Rev. Lett. **65**, 2294 (1990).